CENTRE FOR **STOCHASTIC GEOMETRY**
AND ADVANCED **BIOIMAGING**

Stine Hasselholt, Ute Hahn, Eva B. Vedel Jensen and Jens Randel Nyengaard

Practical implementation of the planar and spatial rotator in a complex tissue – the brain

No. 09, December 2018

Publication metadata

Title:	*Practical implementation of the planar and spatial rotator in a complex tissue: the brain*
Author(s):	*S. HASSELHOLT, U. HAHN, E. B. VEDEL JENSEN, J. R. NYENGAARD*
Journal:	*Journal of Microscopy*
DOI/Link:	https://doi.org/10.1111/jmi.12757
Document version:	Submitted manuscript (pre-print)

Practical implementation of the planar and spatial rotator in a complex tissue – the brain

Stine Hasselholt[1,2,3], Ute Hahn[1,4], Eva B. Vedel Jensen[1,4] and Jens Randel Nyengaard[1,2,3]

[1]Centre for Stochastic Geometry and Advanced Bioimaging, Aarhus University
[2]Section for Stereology and Microscopy, Department of Clinical Medicine, Aarhus University
[3]Sino-Danish Center for Education and Research (SDC)
[4]Department of Mathematics, Aarhus University

Abstract

In neuroscience, application of widely used stereological local volume estimators, including the planar rotator, is challenged by the combination of a complex tissue organisation and an estimator requirement of either isotropic or vertical sections, i.e. randomly oriented tissue. The spatial rotator is applicable with any tissue orientation but is sensitive to projection artefacts. The challenge is thus to select the most appropriate method for individual analyses.

In this study, agreement between estimates of cell volume acquired with the vertical planar and the spatial rotator is assessed for two brain regions with different types of cytoarchitecture (motor cortex and hippocampal cornu ammonis 1). The possibility of using the planar rotator in tissues cut in an arbitrary direction is explored and requirements for a theoretically unbiased result as well as histological considerations are provided.

Abstract 2 – lay description. Cells may change volume both during disease and with advancing age. Assessment of the volume of individual cells can therefore serve as a useful indicator of general tissue state. Most available methods to estimate cell volume in tissue sections, however, require that the tissue analysed has random orientation. Particularly for complex tissues such as the brain this is a challenge as identification, delineation, and subdivision of many brain areas rely heavily on the use of anatomical atlases where illustrations depict the tissue in a few well-known orientations. In this study, the practical application of two different methods for estimating mean cell volumes in tissues cut in a preferred orientation is evaluated. Requirements for the feasibility of cell volume estimation without random tissue orientation as well as histological considerations are provided.

Keywords: cell volume, brain, planar rotator, spatial rotator, rotational invariance.

Corresponding author: Stine Hasselholt, stha@clin.au.dk

1 Introduction

In many tissues including the brain, changes in cell volumes can occur in pathological conditions as well as with age (Overgaard Larsen et al., 1994; Bundgaard et al., 2001; Jansen et al., 2007; Rudow et al., 2008). The ability to assess volume changes locally in the brain provides an opportunity to detect subtle alterations in tissue state while they may still be reversible and is therefore useful in the study of brain disorders. Several stereological probes have been developed for the estimation of number weighted mean cell volume; the nucleator (Gundersen, 1988), the planar rotator (Cruz-Orive, 1987; Jensen and Gundersen, 1993), the optical rotator (Tandrup et al., 1997), the invariator (Cruz-Orive, 2005), and the spatial rotator (Rasmusson et al., 2013). All these geometric probes require an isotropic interaction with the structure under study. As biological specimens are usually anisotropic, the isotropic interaction needs to be obtained either by using a virtual isotropic probe in tissue sections made in any preferred orientation or alternatively, by using isotropic (Mattfeldt et al., 1990; Nyengaard and Gundersen, 1992) or vertical uniform random (VUR) (Baddeley et al., 1986) tissue sections with a randomly oriented probe.

The complexity of the brain makes the practical application of stereological estimators that require randomly oriented tissues difficult. Identification, delineation, and subdivision of numerous brain areas rely heavily on the use of anatomical atlases and cytoarchitectonic features, and the available information is predominantly based on the study of sections with well-known orientations. The spatial rotator requires computer-assisted microscopy but is applicable with any tissue orientation as it is a virtual three-dimensional probe (Rasmusson et al., 2013). Unfortunately, this estimator is sensitive to projection artefacts due to the collection of information in several focal planes within the same cell. It would therefore be advantageous if it was possible to apply a stereological probe using information from a single focal plane in the central part of the cell, like the planar rotator, on brain sections cut in a preferred orientation.

In this study, the practical applicability of the planar and spatial rotator for estimation of mean cell volume in brain sections cut with arbitrary orientation was evaluated. The obtained knowledge about how the magnitude of the bias introduced when using the planar or spatial rotator in sections with a non-random orientation depends on the subregion of the brain studied, provides a more solid foundation for applying local volume probes in complex tissue such as the brain.

2 Materials and methods

Two adult (12 weeks), male, clinically healthy C57BL/6J mice (Taconic, Bomholt, Denmark) were anaesthetised with isoflurane and given 0.05 ml pentobarbital i.p. (Exagon Vet., 400 mg/ml pentobarbital, Salfarm, Denmark). Following a thoracotomy, i.c. perfusion was performed with phosphate buffered saline (PBS) (pH 7.4) for 1 min and 4 % paraformaldehyde in PBS (pH 7.4) for 5 min (flow 5 ml/min). Brains were post fixed by immersion in the same fixative for 24 hours, stored in 1 % paraformaldehyde in PBS (pH 7.4), and processed after less than 7 days.

2.1 Generation of VUR and coronal sections

To generate both VUR and coronal sections from a complex tissue like the brain without loss of orientation, a principle for tissue processing described in (Dorph-Petersen, 1999) was modified for mouse brain and applied. Brains were divided in hemispheres with a cut through the cerebral longitudinal fissure, the cerebellum was removed with a coronal cut at the caudal border of the cerebrum, and a random hemisphere embedded in 5 % agar. A vertical axis (VA) parallel to the rostro-caudal axis of the brain was selected, 1 mm coronal slabs were made using a razor array, and slabs containing motor cortex (M) and hippocampus (Hip), respectively, were assigned alternatingly to coronal and VUR processing, see Figure 1.

2.1.1 Coronal slabs

Slabs were placed on an even surface and re-embedded in 5 % agar, so the surface of the tissue slab was at level with the top surface of the agar block when mounted on the tissue holder for the vibratome.

2.1.2 VUR bars

Slabs were placed randomly within a circle grid, where the circumference is divided in equidistant arcs by numbered diameter lines, and cut in 2 mm bars using a razor array. The cutting direction was specified using a random number table and the corresponding diameter line on the grid. This is equivalent to rotating the tissue randomly around the selected VA. Bars containing M and Hip were re-embedded in 5 % agar with a vertical edge, i.e. a side of the bar parallel to the VA, parallel with the top surface of the agar block, see Figure 1. Thick (80 µm) vibratome sections (LeicaVT1200S, Leica Biosystems, Nussloch, DE) made from both coronal slabs and VUR bars were stored in PBS (pH 7.4) at 4 °C.

2.2 Thionin staining

Sections were mounted on SuperFrost glass slides (Menzel-Gläser, Braunschweig, DE) using 0.5 % Gelatine (CAS 9000-70-8, Sigma-Aldrich, Steinheim, DE) + 0.05 % Chromalun ($CrK(SO_4)_2$, 12 H_2O, BDH Chemicals Ltd, Poole, UK), dried at room temperature for 20 min, and rehydrated in dH_2O for 15 min. The tissues were stained for 60 sec in 0.25 % thionin ($C_{12}H_9N_3S \cdot C_2H_4O_2$, CAS 78338-22-4, Sigma-Aldrich, St. Louis, Missouri, USA), rinsed 5 sec in dH_2O, and dehydrated in a graded series of ethanol solutions (1 min in 70 %, 2 min in 96 %, 5 min in 99 %). Finally, sections were cleared for 3×5 min in xylene and cover slips (No. 0, Hounisen, Skanderborg, DK) mounted using Eukitt® Quick-hardening mounting medium (CAS 25608-33-7, Sigma-Aldrich, Steinheim, DE).

2.2.1 Stain penetration

Thionin stain penetration through sections was assessed with a z-axis analysis on the pyramidal cell layer of the cornu ammonis (CA) 1 region of Hip. Fields of view

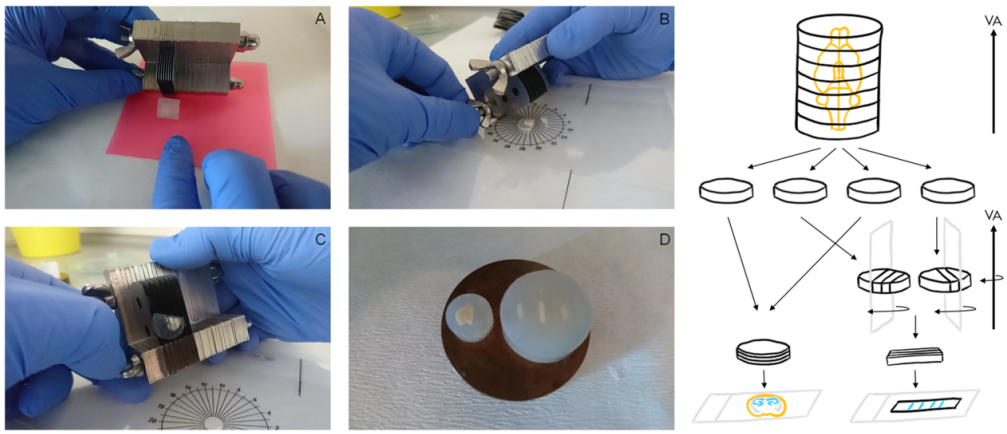

Figure 1 Tissue processing. After fixation, hemispheres were embedded in agar and cut in 1 mm coronal slabs perpendicular to the chosen vertical axis (VA) using a razor array (A). Slabs were alternately allocated for coronal and vertical uniform random (VUR) sectioning, respectively. VUR slabs were randomly rotated around the VA and cut into 2 mm bars with systematic uniform random position (B and C). Both coronal slabs and VUR bars were re-embedded in agar (D) and cut into 80 µm sections perpendicular to or parallel with the VA, respectively, before staining. The illustration is modified from figure 1 in (Dorph-Petersen, 1999).

were sampled systematic uniform random with x- and y-steps of 150 µm, individual pyramidal cells sampled based on position in relation to an unbiased counting frame with area 600 µm^2, and the position of their nuclear centres in the whole z-axis/height relative to the section surface recorded along with the local section thickness.

2.3 Stereological analysis

Initially, cells were sampled number weighted for analysis using the optical disector (Gundersen, 1986). Volume estimates for individual neurons were acquired using the planar rotator for VUR sections (Cruz-Orive, 1987; Jensen and Gundersen, 1993) and spatial rotator (Rasmusson et al., 2013), respectively. For the planar rotator, volume estimates are based on measurements on a grid of parallel test lines (five half lines applied here) perpendicular to the global VA (Jensen and Gundersen, 1993). For the spatial rotator, systematic test rays (five used here, one in each of five focal planes) perpendicular to a local arbitrary VA are used. In practice, the user determines the intersection between test lines/rays and the boundary of the cell profile in one or several focal planes depending on the estimator, see Figure 2 A–C.

Sections were analysed on a Leica microscope (DM6000 B, Leica Microsystems GmbH, Wetzlar, DE) equipped with a Ludl motorized x–y specimen stage (99S121, LUDL Electronic Products LTD., Hawthorne, New York, USA), and an Olympus DP72 digital colour camera (12.8 megapixel, Olympus Denmark, Ballerup, DK). Delineation of the region of interest (ROI) was performed using a 10× objective

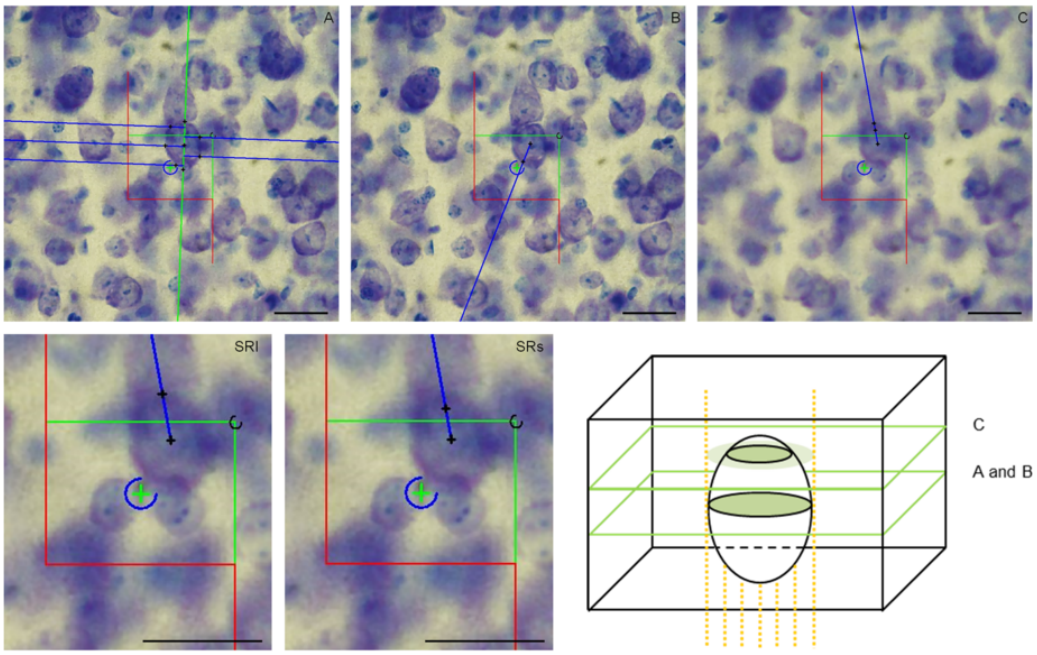

Figure 2 Probes and projection artefacts. For measurements with the planar rotator, a grid of parallel test lines is superimposed on the cell profile in a single central focal plane in the cell (A). Applying the spatial rotator probe, a single test ray is superimposed on the cell profile in each of five different focal planes in the cell and both central (B) and peripheral (C) focal planes are used. In peripheral focal planes of cells, projection artefacts can challenge clear identification of the intersection point between test rays and cell boundary. For the analysis of motor cortex, two different intersection points, SRl and SRs, were therefore used for the spatial rotator (See the digital magnifications of C denoted SRl and SRs). The sampling of focal planes along the z-axis of the cell is indicated in the illustration in the lower right corner. Images A and B are from a central focal plane while image C is from a more peripheral focal plane in the cell. The occurrence of a projection artefact at level C is indicated in light green. The scale bar is 25 µm in all images.

(HCX FL PLAN, NA 0.25, Leica) and the analyses were with a 63× oil objective (HCX PL FLUOTAR, NA 1.25, Leica). Delineations used are in accordance with (Paxinos and Franklin, 2001). For the pyramidal cell layer in the CA1 region of Hip delineations of borders towards CA2-3 and subiculum were furthermore based on (West et al., 1991). For M, sections from genu corpus callosum to the appearance of hippocampus in the rostro-caudal direction were included. Layer V corticospinal motor neurons (CSMN) were analysed and since the primary and secondary motor cortices (M1+M2) are not clearly distinguished cytoarchitectonically in the mouse (Young et al., 2012) both were included in the same ROI.

2.3.1 Parameters

With newCAST software (Ver. 6.4.1.2240, Visiopharm, Hørsholm, DK), fields of view were sampled systematic uniform random in the ROI. Please find the applied parameters in Table 1.

Table 1 Parameter settings. Presented are the parameter settings applied in the newCAST software. CA1; cornu ammonis 1, M1+M2; primary and secondary motor cortices, VUR; vertical uniform random, a(frame); area of the counting frame, h(dis); disector height, x-step and y-step denote the distance in x-y between fields of view analysed.

Region	Tissue orientation	a(frame) (µm^2)	x-step = y-step (µm)	h(dis) (µm)
CA1	Coronal	600 (28.23 × 21.25)	200 × 200	20 (−5 to −25)
	VUR	600 (28.23 × 21.25)	40 × 40 (mouse 1) 75 × 75 (mouse 2)	20 (−5 to −25)
M1+M2	Coronal	1200 (39.92 × 30.06)	100 × 100	20 (−5 to −25)
	VUR	1200 (39.92 × 30.06)	100 × 100	20 (−5 to −25)

2.3.2 Counting criteria

Only clear Thio+ cells with a visible soma border were included in the analysis. Using the unbiased counting frame (Gundersen, 1977) for cell selection, cells were in- or excluded from the analysis based on the position of their nucleus in relation to the frame. If any part of a counting frame was inside the ROI, cells belonging to the frame were analysed. At borders to CA3-2 and subiculum or medial prefrontal- and somatosensory cortices, respectively, cells were only included in the analysis if $> \frac{1}{2}$ their nucleus was inside ROI.

The middle of the cell soma – in the focal plane where the nucleus was largest when focusing from top to bottom of disector – was used as the reference point in the cell. The centre used was annotated in newCAST, so the same centre position could be used for both local probes. When test lines/rays on a cell profile fell inside cell processes (i.e. the direction of the test line/ray and the cell process was relatively

similar), an arc connecting the cell boundary on either side of the process was eyeballed and the soma border set to be where the test lines/rays intersected with the arc.

2.3.3 Estimates

In coronal sections, the following estimates were determined for each cell:

(a) Estimates of cell volume acquired with the planar rotator using two (CA1) or three (M1+M2) different fictive VA. No VA is optimal for all cells in a structure. The selected global VA for CA1 were chosen to be perpendicular to the brain surface following the general cell orientation in the middle of the ROI (denoted A) and parallel to the cerebral longitudinal fissure (denoted B), respectively. For M1+M2 a third VA parallel to the brain surface above the ROI was chosen (denoted C) in addition to the ones used for CA1, see Figure 3.

(b) Estimates of cell volume acquired with the spatial rotator. For M1+M2 the spatial rotator was applied twice using the largest and smallest possible cell radius, respectively. More specifically, the intersection between the test ray and the cell border was set to be either at the outer- (denoted l) or inner (denoted s) border of the hazy rim appearing in peripheral focal planes of the cell due to projection artefacts, see Figure 2.

In VUR sections the cell volume was estimated using the planar rotator. The acquired estimates were selected to be gold standard of the study since projection artefacts are minimal in central focal planes of cells, where the measurements are made. Furthermore, the tissues were fulfilling the requirements for the use of the probe regarding randomisation of the orientation.

2.4 Statistics

The statistical analysis was performed in R (ver. 3.3.2, available from: `https://cran.r-project.org/`, downloaded on 09/05/17). To assess the effect of analysis method on the estimate of cell volume in coronal sections a univariate analysis of variance with random effect of mouse and cell was used for overall effect tests with subsequent Bonferroni corrected t-tests provided significant differences. Where test assumptions were not fulfilled (assessed with raw- and studentized residual plots, and normal qq plots) data transformation was performed. For comparison of cell volumes from coronal sections with the gold standard, planar rotator volumes estimated in VUR sections, unpaired, two-sided Welch t-tests were used followed by Bonferroni correction for multiple comparisons. When the assumption of normally distributed residuals was not fulfilled (assessed with normal qq plots), data transformation or, if needed, a Wilcoxon rank-sum test was performed. A significance level α of 0.05 was used for all calculations.

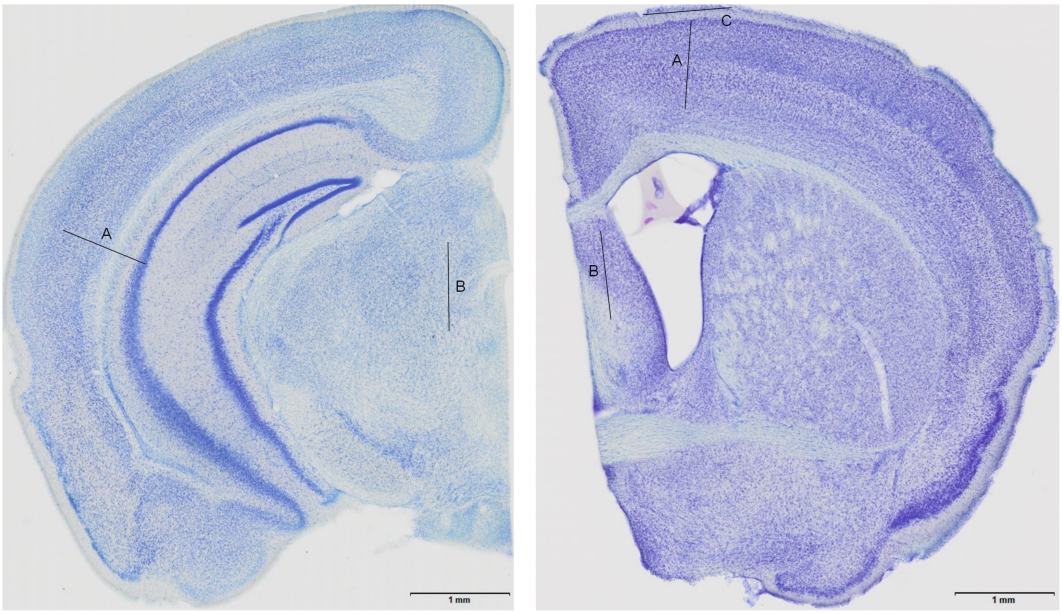

Figure 3 Fictive vertical axes for planar rotator estimates in coronal sections. The selection of global fictive vertical axes for planar rotator estimates in coronal sections is shown. In hippocampal cornu ammonis 1 (left) vertical axes A and B were used. For motor cortex (right), vertical axes A, B, and C were applied.

3 Results

The dataset forming the foundation for the analysis is presented in Table 2. Ambiguous cells were excluded from the analysis.

Table 2 Dataset. m1, m2; mouse 1 and 2, Sect.; section, Amb. of tot.; fraction of ambiguous cells sampled, CA1; cornu ammonis 1, COR; coronal, VUR; vertical uniform random, M1+M2; primary and secondary motor cortices.

Animal	Region	#Sect. or bars	#Disectors	#Cells	Amb. of tot.
m1 + m2	CA1 COR	$7 + 5 = 12$	$65 + 63 = 128$	$147 + 186 = 333$	$6/333 = 0.018$
m1 + m2	CA1 VUR	$10 + 5 = 15$	$45 + 68 = 113$	$140 + 93 = 233$	$2/233 = 0.0086$
m1 + m2	M1+M2 COR	$8 + 7 = 15$	$76 + 65 = 141$	$134 + 122 = 256$	$4/256 = 0.016$
m1	M1+M2 VUR	7	114	212	$5/212 = 0.024$

3.1 Z-axis analysis

The penetration of thionin stain through the sections was good, see Figure 4. Based on the z-axis analysis, the disector used in the study was placed in the interval 5 µm to 25 µm from the section surface resulting in a disector height of 20 µm. Heights from a total of 522 cells in 7 sections were registered and the mean section thickness was 34.2 µm.

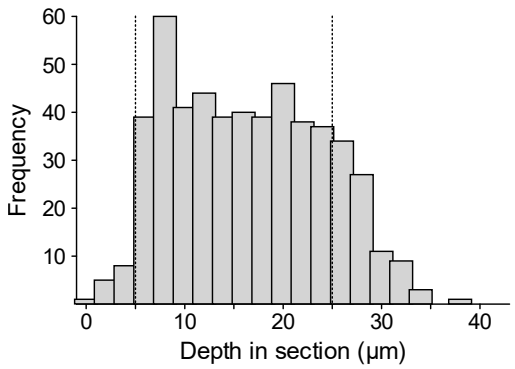

Figure 4 Thionin stain penetration in sections and disector placement. The number of cells counted at different depths in the section is presented. Cells are binned in 2 µm intervals with first interval being −1 to 1. Disector placement is indicated with vertical dotted lines. A total of 522 cells were analysed.

3.2 Hippocampus cornu ammonis 1

3.2.1 Effect of estimator on cell volume in coronal sections

The mean volume estimate for pyramidal cells in Hip CA1 was dependent on the estimator used with the spatial rotator giving a 38 % to 39 % larger estimate than the planar rotator ($p < 0.001$). The two selected fictive VA, A and B, applied with the planar rotator on coronal sections, provided comparable results (1 % difference, see Figure 5).

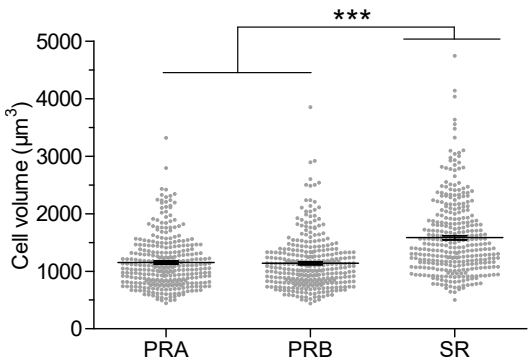

Figure 5 Pyramidal cell volumes in cornu ammonis 1. In coronal sections, the estimates of cell volume depended on the estimator applied. For planar rotator estimates (PRA, PRB), the choice of fictive vertical axes did not affect the mean volume found. Individual measurements are presented together with group means and SEM. PRA; Planar rotator with vertical axis A, PRB; Planar rotator with vertical axis B, SR: Spatial rotator, *** $p < 0.001$

3.2.2 Effect of tissue orientation on mean cell volume

In Hip CA1, planar rotator estimates of mean pyramidal cell volume were comparable in coronal and VUR sections independent of the selected fictive VA for coronal

sections (1 % and 2 % difference to VUR for VA A and B, respectively). The spatial rotator used on coronal sections generally overestimated cell volume when compared with the gold standard planar rotator on VUR sections with a found difference in mean cell volume of 36 % (Figure 6).

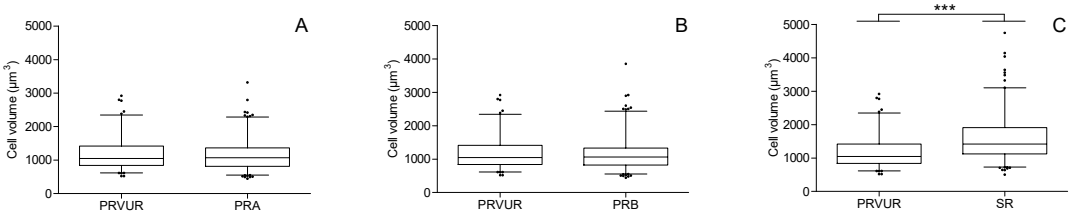

Figure 6 Comparison of pyramidal cell volume estimates in coronal and vertical uniform random sections. A + B) Mean volume estimates acquired with the planar rotator (PRA and PRB, respectively) in coronal sections were comparable with the estimates obtained in vertical uniform random sections. C) Compared with the planar rotator in vertical uniform random sections, the spatial rotator provided a larger estimate of mean cell volume in cornu ammonis 1 of the hippocampus. Boxes depict median, 1st, and 3rd quartiles and whiskers indicate 2.5 and 97.5 percentiles. Extreme values are presented individually. Please note that PRVUR is identical in A–C. PRVUR; Planar rotator in vertical uniform random sections, PRA; Planar rotator with vertical axis A, PRB; Planar rotator with vertical axis B, SR: Spatial rotator, *** $p < 0.001$.

3.3 Motor cortex

3.3.1 Effect of estimator on cell volume in coronal sections

The mean volume estimate for CSMN in layer V of M1+M2 was dependent on the estimator used ($p < 0.001$). The selected fictive VA applied with the planar rotator on coronal sections also affected the estimate (see Figure 7). VA A and B provided similar results (1 % difference) while the mean volume estimate using VA C was 18 % or 20 % higher than A and B estimates, respectively.

3.3.2 Effect of tissue orientation and fictive VA on mean cell volume

Unlike the findings in Hip, the agreement between mean estimates of CSMN volume obtained with the planar rotator in coronal and VUR sections of M1+M2 depended on the selected fictive VA in the coronal sections, Figure 8. Using VA A and VA B, the found mean estimates were 7 % and 8 % smaller than VUR results, respectively, while the mean estimates of CSMN volume when VA C was used was 12 % higher than the VUR estimate. For technical reasons, VUR sections from M1+M2 were only available from mouse 1. To avoid confounding, data from mouse 2 was therefore excluded in the comparative analysis of planar rotator estimates in coronal and VUR sections.

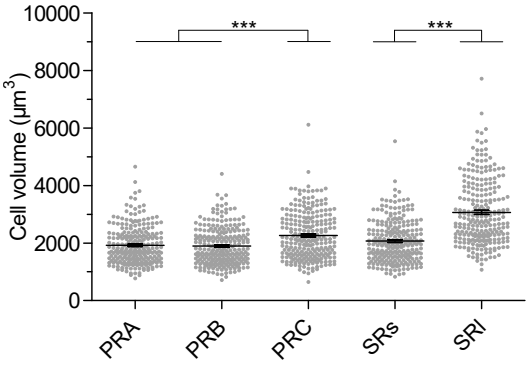

Figure 7 Volumes of corticospinal motor neurons in layer V of motor cortex. In coronal sections, the mean estimates of cell volume depended on the estimator used. For planar rotator estimates (PRA, PRB, PRC) the choice of fictive vertical axis was also of importance. Individual measurements are presented together with group means and SEM. Selected pairwise comparisons are shown. PRA; Planar rotator with vertical axis A, PRB; Planar rotator with vertical axis B, PRC; Planar rotator with vertical axis C, SRs and -l: Spatial rotator used with smallest and largest cell radius, respectively, *** $p < 0.001$.

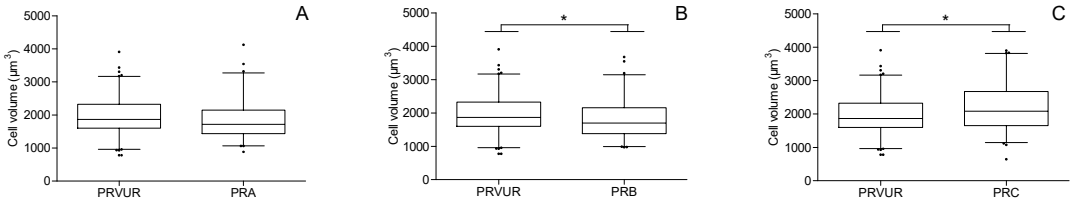

Figure 8 Comparison of corticospinal motor neuron volume estimates in coronal and vertical uniform random sections. A) Mean volume estimates acquired with the planar rotator in coronal and vertical uniform random sections were comparable, when fictive vertical axes A was selected. B+C) When using fictive vertical axes B and C (PRB and PRC, respectively), planar rotator estimates of mean volume were different in coronal and vertical uniform random sections. Boxes depict median, 1st, and 3rd quartiles and whiskers indicate 2.5 and 97.5 percentiles. Extreme values are presented individually. Please note that PRVUR is identical in A–C and all estimates originate from mouse 1. PRVUR; Planar rotator in vertical uniform random sections, PRA; Planar rotator with vertical axis A, PRB; Planar rotator with vertical axis B, PRC: Planar rotator with vertical axis C, * $p < 0.05$.

3.3.3 Selection of cell boundary for spatial rotator measurements

As seen in Figure 7 and 9, the definition of cell boundary made by the analyser has a massive effect on mean volume estimates acquired with the spatial rotator. When comparing with results from the planar rotator in VUR sections, the spatial rotator used on coronal sections provides a 46 % higher mean CSMN volume (Figure 9 A) if the largest possible cell radius is used and almost similar results (1 % difference was observed) to the planar rotator probe if the smallest possible cell radius is applied (Figure 9 B).

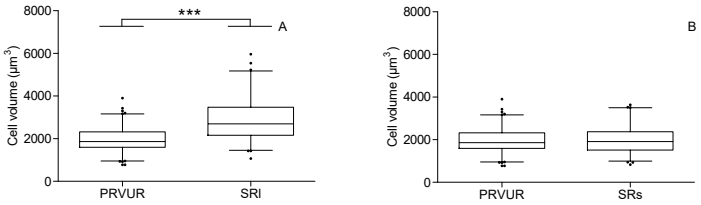

Figure 9 Comparison of planar- and spatial rotator estimates of corticospinal motor neuron volume. Depending on the used cell radius the two estimators provide different (A) or comparable (B) mean estimates of cell volume. Boxes depict median, 1st, and 3rd quartiles and whiskers indicate 2.5 and 97.5 percentiles. Extreme values are presented individually. Please note that PRVUR is identical in A and B and all estimates originate from mouse 1. PRVUR; Planar rotator in vertical uniform random sections, SRl; Spatial rotator used with large cell radius, SRs; Spatial rotator used with small cell radius, *** $p < 0.001$.

4 Discussion

The main finding in the present study was the assessment of the bias of mean volume estimates for specific cell populations in two different brain regions using the planar rotator probe on tissues cut in a preferred orientation, namely coronal. The results indicate the possibility of applying the planar rotator in coronal sections in some brain regions. This extends the range of applications for the planar rotator simplifying the use of the stereological probe in complex tissues.

4.1 Application of the planar rotator

In Hip, the bias arising from using the planar rotator in coronal sections instead of VUR sections was negligible (∼2 %) whereas its magnitude in M1+M2 depended on the chosen fictive VA (7 % to 12 %).

The agreement found between planar rotator estimates of mean pyramidal cell volume in VUR and coronal sections of Hip, independent of the fictive VA chosen in coronal sections, may be at least partly due to the tortuous anatomy of CA1 – and Hip in general – such that CA1 can be considered globally isotropic for practical purposes. In order to investigate this, the analysis was repeated and extended in layer V of M1+M2, where the cytoarchitecture is relatively constant throughout the region and cell orientation is less random than in CA1. Here the choice of VA influenced

the mean volume estimate. This indicates that certain requirements should be met by the tissue under study – more specifically the cell population analysed – for it to be possible to use the planar rotator in sections cut in a preferred orientation.

4.1.1 Rotational invariance

The planar rotator provides an unbiased estimator of mean cell volume if the sections through the reference points of the sampled cells have a uniform rotation around a specified VA. For each sampled cell, the VA is positioned such that it passes through the reference point of the cell and measurements are performed relative to this axis (Jensen and Gundersen, 1993).

However, unbiasedness may still be achieved, using sections with a fixed orientation (in this study coronal), if the cell population under study fulfils the assumption of rotational invariance. To explain what this means, imagine that each of the cells in the population is equipped with a VA through its reference point. All these local VA are parallel. Then, section each of the cells with a vertical plane, i.e. a plane containing the VA. All these local vertical planes are parallel with common rotation angle θ, relative to a reference plane. Consider all the section profiles between the cells and their local vertical planes. A cell population satisfies the rotational invariance assumption if the distribution of size, orientation, and shape of the profiles does not depend on the rotation angle θ.

As an example, consider a cell population where all cells have the same size and shape, being prolate ellipsoids with the longest axis parallel to the z-axis (see Figure 10 A). This cell population satisfies the rotational invariance assumption if the VA is chosen to be the z-axis. For all rotation angles θ around VA, all cell profiles are ellipses (compare the green and blue profile plots in Figure 10 A left). However, the assumption is not fulfilled if the VA is the x-axis, say. Thus, if the local vertical planes are all parallel to the xy-plane, all profiles are circular disks, while if the local vertical planes are all parallel to the xz-plane, all profiles are ellipses (compare the green and blue profile plots related to Figure 10 A right).

In the two brain regions CA1 and M1+M2, the two situations presented in Figure 10 A and B are represented. When cells are sampled at random throughout CA1, the orientational distribution of the analysed cell population, as a whole, will resemble the ellipsoids in Figure 10 B and the assumption of rotational invariance is fulfilled, irrespectively of the choice of VA. In contrast, in layer V of M1+M2 the orientation of the cell population resembles the ellipsoids in Figure 10 A. The assumption of rotational invariance is not fulfilled for all VA, explaining the bias observed when using the planar rotator on coronal sections of M1+M2.

To evaluate whether a cell population analysed is rotational invariant, knowledge about the cytoarchitecture in the ROI as well as the neuroanatomy of the structure is beneficial. Together with a pilot study resembling the one performed here, an indication of the cell organization can be acquired. If this is not possible, VUR sections are needed.

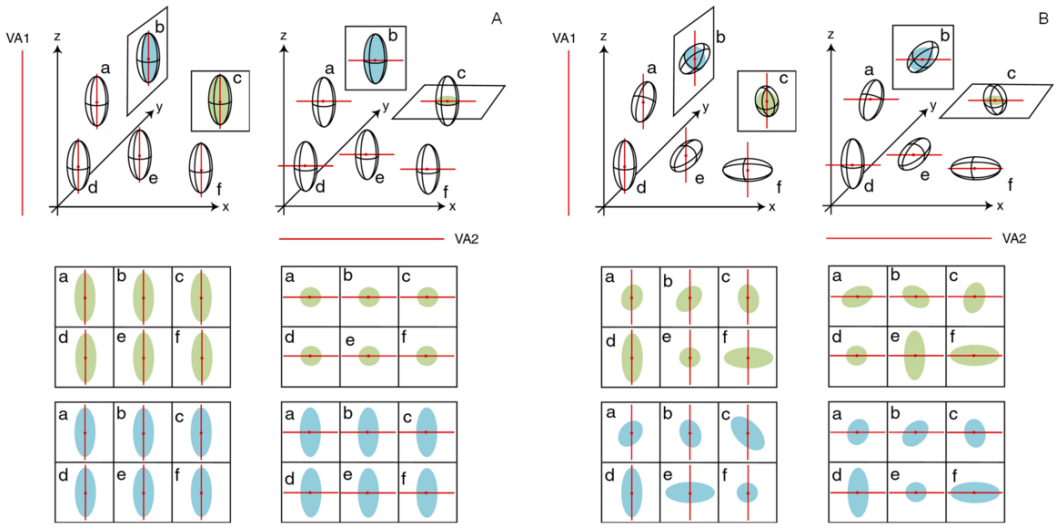

Figure 10 Rotational invariance. Application of the planar rotator in sections cut in a preferred orientation requires an assumption of rotational invariance. For a cell population to be rotational invariant, the distribution of size, orientation, and shape of section profiles analysed should be unchanged when changing the cutting direction of the tissue – as long as the direction is parallel with the selected fictive vertical axis (VA). This is the case in illustration A left, where the VA is chosen to be the z-axis. As seen in the two profile plots, all cell profiles are ellipses of the same size, orientation, and shape independent of the rotation angle of the vertical plane. However, as seen in illustration A right, if the fictive VA is selected to be the x-axis, the cell population is no longer rotational invariant. For some cutting directions, the cell profiles will be ellipses whereas the profiles are circular discs for other cutting directions. Thus, the selected fictive VA is of importance for fulfilment of the rotational invariance assumption related to the planar rotator. In illustration B left and right, the cell population is rotational invariant independent of the chosen fictive VA. The distribution of size, orientation, and shape of cell profiles is similar for all selected VA.

4.2 Application of the spatial rotator

The precision of spatial rotator estimates when compared to the selected gold standard was considerably affected by regional cytoarchitecture, quality of staining, and correct identification of the intersection between test rays and cell profile boundary. Unlike in Hip, it was in M1+M2 possible to distinguish the outer and inner border of a hazy rim at the cell boundary appearing in peripheral focal planes of the cell. Consequently, two volume estimates were determined for each cell with the spatial rotator in coronal sections, to assess the correct choice of cell boundary based on a comparison with planar rotator measurements in VUR sections.

Since both estimators are unbiased (Jensen and Gundersen, 1993; Rasmusson et al., 2013) bias in spatial rotator measurements is likely to be caused by over- and underprojection (Rasmusson et al., 2013). The effect of using either the large (outer rim) or small (inner rim) boundary was substantial and the accompanying bias decreased from 46 % to 1 % when using the small boundary. In the original article presenting the spatial rotator, a bias of 10 % was found when the same two estimators were compared (Rasmusson et al., 2013). Their comparison is more sophisticated in the sense that they analysed the same cells using both estimators in isotropic uniform random sections, whereas mean estimates acquired from VUR and coronal sections for the planar and spatial rotator, respectively, were compared here. On the other hand, the analysis performed here provides information about the practical application of the spatial rotator in sections with a preferred orientation. Rasmusson et al. (2013) studied the subiculum where the cell density is in between the ones found in CA1 and M1+M2 layer V, so it may have been possible to identify the projection artefacts in this brain region and adjust the selection of intersection between estimator test rays and cell boundary accordingly. If not, this may be part of the explanation for the difference in bias magnitude seen. Whether or not it is possible to see projection artefacts clearly depends on cell density, quality of the stain and intensity differences between cells and the extracellular matrix. The spatial rotator may be usable in tissues with light extracellular matrix and low cell density. Here, it is easier to define cell borders in focal planes at the top and bottom of the cell. Furthermore, its use is facilitated by the increased resolution in individual focal planes in more advanced microscopes.

For both probes, a clear definition of cell boundary becomes a challenge if the cell density is high. However, due to the use of only a single, central focal plane for planar rotator measurements, the situation is more manageable here. In Table 3, cautious recommendations for the practical application of the two local stereological probes evaluated here are presented.

4.3 Precision of acquired estimates of mean cell volume

A limitation of the current study is the small number of animals and therefore number of brain slabs available from the different regions analysed, due to the limited size of the mouse brain and the simultaneous use of hemispheres for production of both coronal and VUR sections. Consequently, it was only possible to make tissue with a few rotations around the VA for VUR analysis (for M1+M2 only one). Additionally, although a suitable immersion medium was used between the specimen

Table 3 Overview of probe requirements and recommendations for practical application. ECM: Extracellular matrix, ROI: Region of interest, VA: Vertical axis, VUR: Vertical Uniform Random.

	Planar rotator (original)	Planar rotator (new suggestion)	Spatial rotator
Section orientation	Isotropic, VUR	Any	Any
Probe orientation in section	Any	Any	Isotropic
Cell density	Medium-High	Medium-High	Low
Cytoarchitecture/ neuroanatomy	No requirements	Rotational invariance	No requirements
Staining	Better quality needed for high density	Better quality needed for high density	High quality, contrast between cell and ECM large
Challenge	Identification of ROI		Identification of cell boundary

and the objective, a refractive mismatch may be present as no immersion medium was applied between the condenser and the specimen. Most likely, this would have improved the resolution of the live image, potentially minimizing the magnitude of the bias particularly for the spatial rotator.

In summary, in some situations the planar rotator may provide valid estimates of mean cell volume in sections cut in a preferred orientation as well as in isotropic and VUR sections. The applicability in coronal sections depends on neuroanatomy and cytoarchitecture in the ROI and it is recommended always to perform a pilot study for brain areas with which the researcher is unfamiliar. The spatial rotator is probably not the estimator of choice for regions with high cell density. It can be an alternative to the planar rotator in brain regions without rotational invariance. Practice is needed to determine the intersection between test rays and cell boundary in top- and bottom focal planes of a cell and the use of the estimator requires a high quality of staining and the use of a microscope with an acceptable resolution in the z-axis.

5 Acknowledgements

The authors wish to thank Helene Andersen and Kaj Vedel for invaluable technical assistance with tissue preparation and graphical illustrations, respectively. This project was supported by Centre for Stochastic Geometry and Advanced Bioimaging funded by a grant from the Villum Foundation, Sino-Danish Center for Education and Research, and 'Henny Sophie Clausen og møbelarkitekt Aksel Clausens Fond'.

References

Baddeley, A. J., Gundersen, H. J., and Cruz-Orive, L. M. (1986). Estimation of Surface-Area from Vertical Sections. *J Microsc*, **142**, 259–276.

Bundgaard, M. J., Regeur, L., Gundersen, H. J., and Pakkenberg, B. (2001). Size of neocortical neurons in control subjects and in Alzheimer's disease. *J Anat*, **198**, 481–889.

Cruz-Orive, L. M. (1987). Stereology: recent solutions to old problems and a glimpse into the future. In: *Proc. 7th Int. Congr. for Stereology, Acta Stereol*, (ed. J.-L. Chermant). Plešco, Ljubljana, Yugoslavia.

Cruz-Orive, L. M. (2005). A new stereological principle for test lines in three-dimensional space. *J Microsc*, **219**, 18–28.

Dorph-Petersen, K. A. (1999). Stereological estimation using vertical sections in a complex tissue. *J Microsc*, **195**, 79–86.

Gundersen, H. J. (1977). Notes on the estimation of the nummerical density of arbitrary profiles: the edge effect. *J Microsc*, **111**, 219–223.

Gundersen, H. J. (1986). Stereology of arbitrary particles. A review of unbiased number and size estimators and the presentation of some new ones, in memory of William R. Thompson. *J Microsc*, **143**, 3–45.

Gundersen, H. J. (1988). The nucleator. *J Microsc*, **151**, 3–21.

Jansen, P., Giehl, K., Nyengaard, J. R., Teng, K., Lioubinski, O., Sjoegaard, S. S., Breiderhoff, T., Gotthardt, M., Lin, F., Eilers, A., Petersen, C. M., Lewin, G. R., Hempstead, B. L., Willnow, T. E., and Nykjaer, A. (2007). Roles for the pro-neurotrophin receptor sortilin in neuronal development, aging and brain injury. *Nat Neurosci*, **10**, 1449–1457.

Jensen, E. B. V. and Gundersen, H. J. (1993). The Rotator. *J Microsc*, **170**, 35–44.

Mattfeldt, T., Mall, G., Gharehbaghi, H., and Möller, P. (1990). Estimation of surface-area and length with the orientator. *J Microsc*, **159**, 301–317.

Nyengaard, J. R. and Gundersen, H. J. (1992). The isector – a simple and direct method for generating isotropic, uniform random sections from small specimens. *J Microsc*, **165**, 427–431.

Overgaard Larsen, J., Tandrup, T., and Braendgaard, H. (1994). The volume of Purkinje cells decreases in the cerebellum of acrylamide-intoxicated rats, but no cells are lost. *Acta Neuropathol*, **88**, 307–312.

Paxinos, G. and Franklin, K. B. J. (2001). *The Mouse Brain in Stereotaxic Coordinates*. Academic Press: San Diego, California, USA.

Rasmusson, A., Hahn, U., Larsen, J. O., Gundersen, H. J., Jensen, E. B. V., and Nyengaard, J. R. (2013). The spatial rotator. *J Microsc*, **250**, 88–100.

Rudow, G., O'Brien, R., Savonenko, A. V., Resnick, S. M., Zonderman, A. B., Pletnikova, O., Marsh, L., Dawson, T. M., Crain, B. J., West, M. J., and Troncoso, J. C. (2008). Morphometry of the human substantia nigra in ageing and Parkinson's disease. *Acta Neuropathol*, **115**, 461–470.

Tandrup, T., Gundersen, H. J., and Jensen, E. B. (1997). The optical rotator. *J Microsc*, **186**, 108–120.

West, M. J., Slomianka, L., and Gundersen, H. J. (1991). Unbiased stereological estimation of the total number of neurons in thesubdivisions of the rat hippocampus using the optical fractionator. *Anat Rec*, **231**, 482–497.

Young, N., Stepniewska, I., and Kaas, J. (2012). Motor Cortex. In: *The Mouse Nervous System* (eds. C. Watson, G. Paxinos, and L. Puelles). Academic Press: San Diego, California, USA, 528–538.